MOLECULAR AND CELLULAR BIOLOGY, Aug. 2004, p. 7113–7129 Vol. 24, No. 16
0270-7306/04/$08.00+0 DOI: 10.1128/MCB.24.16.7113–7129.2004

Defective Extraembryonic Angiogenesis in Mice Lacking LBP-1a, a Member of the grainyhead Family of Transcription Factors

Vishwas Parekh,[1] Amy McEwen,[1] Virginia Barbour,[1] Yutaka Takahashi,[2] Jerold E. Rehg,[3] Stephen M. Jane,[4] and John M. Cunningham[1,5]*

Departments of Hematology/Oncology,[1] Biochemistry,[2] and Pathology,[3] St. Jude Children's Research Hospital, and Departments of Molecular Sciences and Pediatrics,[5] University of Tennessee, Memphis, Tennessee 38105, and Rotary Bone Marrow Research Laboratory, Royal Melbourne Hospital Research Foundation, Parkville, Victoria 3050, Australia[4]

Received 20 October 2003/Returned for modification 3 January 2004/Accepted 3 May 2004

LBP-1a and CP2 are ubiquitously expressed members of the grainyhead transcription factor family, sharing significant sequence homology, a common DNA binding motif, and modulating a range of key regulatory and structural genes. We have reported previously that CP2-null mice are viable with no obvious abnormality. LBP-1a provides redundant function in this context. We show here that mice lacking LBP-1a expression develop intrauterine growth retardation at embryonic day 10.5, culminating in death 1 day later. No focal intraembryonic cause for this CP2-independent defect is evident. In contrast, a significant reduction in the thickness of the labyrinthine layer of the placenta is observed in LBP-1a$^{-/-}$ animals. However, expression of trophoblast differentiation markers is unperturbed in this context, and complementation studies utilizing tetraploid wild-type cells failed to rescue or ameliorate the LBP-1a$^{-/-}$ phenotype, excluding a primary trophoblast defect. An explanation for these observations is provided by the prominent angiogenic defect observed in the mutant placentas. LBP-1a$^{-/-}$ allantoic blood vessels fail to penetrate deeply and branch into the complex embryonic vasculature characteristic of the normal placenta. Interestingly, a similar defect in angiogenesis is observed in the yolk sac vasculature, primary endothelial cell-lined capillary tubes, although present, failed to connect into a characteristic intricate vascular network. Collectively, these results demonstrate that LBP-1a plays a critical role in the regulation of extraembryonic angiogenesis.

Prior to embryonic day 9.5 (E9.5), the normal murine embryo can survive by direct exchange of gases, nutrients, and toxic metabolites with the surrounding amniotic fluid. Subsequently, the intermingling of maternal blood sinuses with the extraembryonic vasculature in the placenta is critical for effective feto-maternal exchange. To facilitate this process, extraembryonic trophoectoderm cells and allantoic mesoderm undergo a complex series of complementary differentiation events, resulting in a mature chorioallantoic placenta (35). Gene disruption studies have provided significant insights into the tissue-specific and ubiquitously expressed regulators of choriotrophoblast ontogeny. Among others, the Mash-2 (15), Dlx3 (28), SOCS3 (45), and Gcm1a (3) transactivators, the fibroblast growth factor (FGF) (52), Frizzled (19), and Met (11) growth factor receptors, cell adhesion molecules such as VCAM (16) and integrin α4 (53), and the intracellular signaling molecules Gab1 (20) and mitogen-activated protein kinases (1, 13) have been identified as key regulators of this process. In this context, replacement of the factor-deficient placenta with wild-type trophoblasts by tetraploid complementation (15) results in correction and/or amelioration of the phenotype.

In contrast, disruption of genes necessary for appropriate development of the extraembryonic allantoic-vitelline vasculature presents frequently with a similar phenotype but cannot be rescued by tetraploid complementation (49). Indeed, the critical need for appropriate formation of the allantoic and yolk sac vasculature at midgestation is emphasized by the defects in embryonic and extraembryonic development observed with loss of vascular-specific growth factor and transactivator expression. For example, the vascular endothelial growth factor (VEGF) (9, 12, 40) and transforming growth factor β (TGF-β)/bone morphogenetic protein (BMP) families of factors and their receptors (7, 10, 23, 24, 31, 42, 54) and coreceptors are required for extraembryonic vasculogenesis. This process is development restricted and encompasses initial endothelial cell differentiation from hemangioblast stem cells and the formation of a primary plexus of homogeneously sized capillary tubes. Defects in vasculogenesis are usually manifest around E7.5 and are associated frequently with defects in primitive hematopoiesis, a result of the common hemangioblast origin of these cell types (15).

In contrast to the purely developmental nature of vasculogenesis, angiogenesis is required pre- and postnatally. Angiogenesis involves endothelial tube remodeling with recruitment and/or differentiation of perivascular cells and branching morphogenesis. Members of the VEGF, TGF-β/BMP, *wingless*-related (Wnt) (27, 32), FGF (45), platelet-derived growth factor (29, 30), and hedgehog (5) families, among others, have been implicated in this process. Defective angiogenesis may cause embryonic lethality between E9.5 and birth and is associated frequently with labyrinthine defects and severe intrauterine fetal growth retardation.

A *Drosophila* homologue of the TGF-β/BMP growth factor gene family, *decapentaplegic*, is repressed, like other early patterning genes, by *grainyhead* (*grh*), a transacting factor gene

* Corresponding author. Mailing address: Department of Hematology/Oncology, St. Jude Children's Research Hospital, 332 N. Lauderdale, Memphis, TN 38105. Phone: (901) 495-2746. Fax: (901) 495-2176. E-mail: john.cunningham@stjude.org.

with a unique DNA-binding domain (4, 18). Six mammalian homologues of *grh* and a highly related orthologue (*dCP2*) have been identified (46, 51). Of these, the function(s) of two widely expressed mammalian homologues, CP2/LBP1c/LSF and LBP-1a/NF2d9 (referred to as LBP-1a here) have been evaluated extensively in cellular models (41, 48). Both factors are expressed ubiquitously, have little variation in tissue expression, and share a high degree of amino acid identity (72%) and similarity (88%), particularly in their DNA-binding and transactivation domains. Homomeric interactions have been implicated in the regulation of both regulatory and structural genes, including the c-*fos*, ornithine decarboxylase, c-*myc*, α-globin, and γ-fibrinogen genes. In contrast, we and others have shown that heteromeric interactions facilitate expression of the γ-globin (21, 55) and steroid 16α-hydroxylase genes (43).

To broaden our understanding of the roles of these factors, we generated mice in which the murine CP2 and LBP-1a genomic loci were disrupted by homologous recombination in murine embryonic stem (ES) cells. Mice homozygous for a deletion of the CP2 locus are viable and have a normal life expectancy (33). We conclude from these studies that LBP-1a provides a redundant function for CP2 in this context, given the high degree of sequence identity, the apparent ability of each factor to substitute in heteromeric interactions, their equivalence of binding to their cognate DNA sequences, and comparable mechanism(s) of transactivation. We hypothesized that targeting of the LBP-1a locus would provide a similar result. To our surprise, LBP-1a$^{-/-}$ mice die at E10.5 of placental insufficiency. Furthermore, our studies provide evidence that an angiogenic defect in the mesodermal components of the labyrinthine layer and the yolk sac vasculature explains the lethal phenotype.

MATERIALS AND METHODS

Gene targeting and genotyping. A BAC clone containing the mouse LBP-1a gene was isolated from a 129SvEv genomic library using a full-length murine cDNA probe specific for LBP-1a. Appropriate restriction fragments were selected for the generation of a targeting construct. The AB2.1 ES cell line was electroporated with the targeting construct, with resultant ES cell clones being screened for homologous recombination by Southern analysis (36) by using unique 5′ and 3′ genomic probes that were outside the sequences encoded by the targeting vector. Several positive clones were karyotyped, and ES cells from three clones were injected into mouse blastocysts according to standard procedure. Chimeric mice were mated with C57BL/6 mice for the generation of F_1 animals, which were further bred to generate F2 progeny. Genomic DNA was isolated from tail clippings at 3 weeks of age or from visceral yolk sacs at various embryonic ages. Genotyping was performed initially by Southern blot analysis and subsequently by PCR (36). The primers used for PCR genotyping were ASM1 (TCCATCATGGCTGATGCAATGCGGC; forward primer for the wild-type and targeted alleles), ASM4 (GCAGAAGCGAAGCCTCAT; reverse primer for the wild-type allele), and ASM14 (GACCAACTCTTGGTTGTTG AGG; reverse primer for the targeted allele). The reaction was carried out on a Perkin-Elmer DNA thermal cycler 480 under the following conditions: initial denaturing at 94°C for 3 min, 30 cycles of denaturing at 94°C for 30 s, annealing at 58°C for 30 s, and extension at 72°C for 3 min, followed by extension at 72°C for 10 min and cooling down to 4°C.

Embryo dissection, histology, and immunohistochemistry. Timed mating between heterozygous animals were established to yield several concepti at various time points in embryonic development. Midday of the plug detection date was considered day 0.5 (E0.5) of pregnancy. Pregnant females were euthanized, and concepti were removed. The uterine wall and Reichter membrane were removed to visualize and photograph the yolk sac vasculature. Embryos and placenta were separated and photographed, while a part of the visceral yolk sac or the embryo was used for the genotyping. For histological analysis, embryos, placentas and yolk sacs were fixed overnight in 4% paraformaldehyde and further processed for paraffin embedding. Serial sections (6 μm) were cut, deparaffinized, and stained with hematoxylin and eosin (H&E) by standard methods. Stained sections of mutant or control embryos and placentas from the same pregnancy were compared in detail and photographed by using a Zeiss microscope.

Whole-mount immunohistochemistry for platelet endothelial cell adhesion molecule (PECAM; Pharmingen) was performed as previously described (39). For VEGF-R2 (R&D Systems) and α-SMA (Sigma) immunostaining of yolk sac, placenta, and embryo sections, slides were incubated in 1% H_2O_2 for 10 min to quench endogenous peroxidases. After being rinsed in phosphate-buffered saline (PBS), they were blocked in phosphate-buffered saline (PBS)–0.1% Triton X-100–5% sheep serum for 30 min, followed by incubation overnight at 4°C in blocking buffer containing VEGF-R2 and α-SMA antibody. After three washes in PBS, slides were incubated for 1 to 2 h in blocking buffer containing the secondary antibody. After a further three washes in PBS, the signal was visualized with diaminobenzidene in PBS containing 0.5% NiCl.

Northern blotting and in situ hybridization analysis. Northern blots were prepared by standard methods and hybridized with randomly primed cDNA probes generated from the 5′ and 3′ ends of LBP-1a mRNA and the 5′ end of CLASP2 mRNA (2). Riboprobes used for in situ hybridization were kindly provided by Janet Rossant (MPL-1, PLF-1, and 4311) (6) and Peter Gruss (HSP-84) (49). Ten-micrometer-thick frozen sections were hybridized with riboprobes by standard procedures, and slides were autoradiographed at 4°C for 3 days. Slides were subsequently coated with photographic emulsion and stored for 2 weeks in the dark prior to development. Slides were counterstained and photographed by using a polarizing microscope.

Tetraploid rescue experiment. Two-cell-stage embryos were flushed from the oviducts of superovulated CD-1 outbred females (Charles River Laboratories) at E1.5 of the pregnancy. The blastomeres were fused by using a CF150B electrofusion apparatus (Biochemical Laboratory Service, Ltd.) as previously described (15). Briefly, two-cell-stage embryos placed in 0.3 M mannitol drops were aligned in a 1.6-V AC field and fused with two 75-V DC pulses of 40 μs each by using a 500-μm electrode. Successfully fused embryos were cultured overnight in drops of KSOM medium (Specialty Media, Inc.) under an embryo-tested light paraffin oil layer (Sigma Laboratories). Eight-cell stage embryos were recovered from the oviducts of E2.5 pregnant LBP-1a heterozygous females mated to LBP-1a heterozygous males. After zona removal, two four-cell-stage tetraploid wild-type embryos and a diploid eight-cell-stage embryo from the heterozygous cross were aggregated overnight, and successfully developed blastocysts were transferred to the uteri of E2.5 pseudopregnant B6cBAF1 recipients. For recovering viable fetuses, cesarean section was performed on E20.5 of gestation, and the fetuses were fostered. After genotypic confirmation that no LBP-1a$^{-/-}$ pups were obtained, embryos and placentas were dissected for analysis at various stages of development in subsequent experiments.

RESULTS

Targeted mutagenesis of the LBP-1a locus results in embryonic lethality. To examine the range of biologic function(s) of the LBP-1a gene, we targeted the LBP-1a allele for disruption by homologous recombination. The targeting strategy, summarized in Fig. 1A, replaced the promoter, exon 1, and part of intron 1 of the LBP-1a gene with a neomycin resistance gene driven by the pyruvate kinase promoter and transcribed in the reverse direction to the targeted gene. ES cell clones in which homologous recombination had occurred were identified by Southern analysis with unique 5′ and 3′ probes (Fig. 1B and data not shown). Three independent ES cell clones were used to generate chimeric mice, with the use of two of three clones resulting in transmission of the LBP-1a mutated allele to its offspring. Both murine cell lines had an identical phenotype. Heterozygous mice were viable, fertile, and phenotypically indistinguishable from wild-type littermates. In matings with wild-type mice, the mutant LBP-1a allele was detected in ca. 50% of the progeny. However, no viable LBP-1a$^{-/-}$ pups were obtained from more than 20 litters derived from heterozygous intercrosses, indicating that mice lacking LBP-1a die during embryogenesis (Fig. 1C).

To identify the developmental stage at which lethality oc-

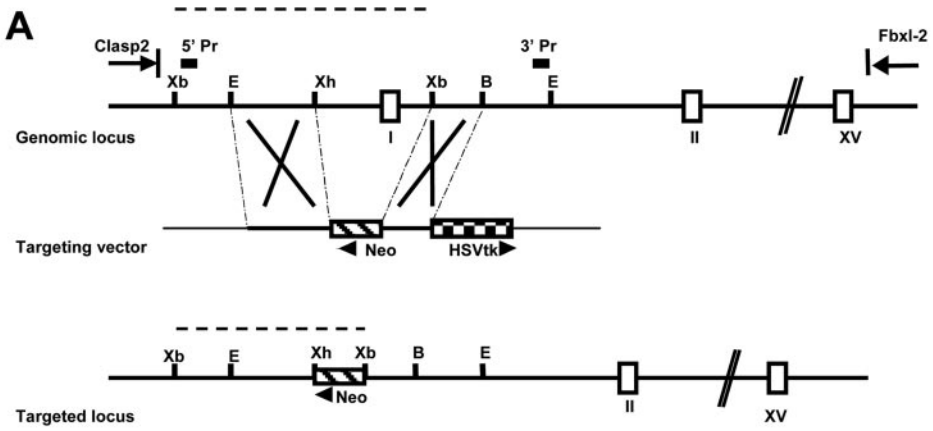

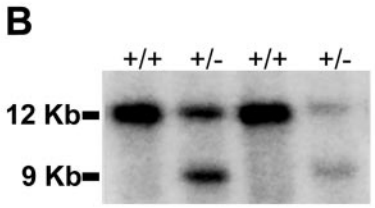

C

Stage	+/+	+/-	-/-	Total
E 8.5	11	10	7	28
E 9.5	49	92	36	177
E 10.0	11	30	10	51
E 10.5	76	102	54	232
E 11.0	2	3	2*	7
E 11.5	40	66	34*	140
E 12.5	22	34	0	56
E 14.5	8	20	0	28
E 15.5	3	7	0	10
3 weeks	78	153	0	231

FIG. 1. Targeted disruption of the murine LBP-1a locus results in embryonic lethality. (A) Schematic representation of the targeting strategy of the LBP-1a gene. The top line represents the genomic locus of LBP-1a, and the open boxes represent exons. The position of the upstream CLASP-2 gene and downstream Fbxl-2 gene are indicated (Parekh and Cunningham, unpublished). The middle line represents the targeting construct. The PGK neomycin phosphotransferase cassette is indicated by a hatched box and the HSVtk negative selection cassette is indicated by a checkered box. Plasmid sequences are indicated by the thinner black line. The bottom line represents the structure of the targeted LBP-1a allele. Restriction sites indicated are those for Xb, XbaI; E, EcoRI; Xh, XhoI; B, BamHI. 5′ and 3′ probes are indicated by filled boxes. The fragment lengths for a diagnostic XbaI digest predicted by using a 5′ probe are indicated by dashed lines. (B) Identification of ES cells carrying a targeted LBP-1a allele. ES DNA digested with XbaI was analyzed by hybridization with the 5′ probe described above. The 12- and 9-kb bands derived from the wild-type LBP-1a gene and the targeted allele, respectively, are indicated on the left. (C) Genotyping statistics of heterozygous intercrosses indicate embryonic lethality just after E10.5 in homozygous mutants. Dead and necrotic embryos are indicated by an asterisk.

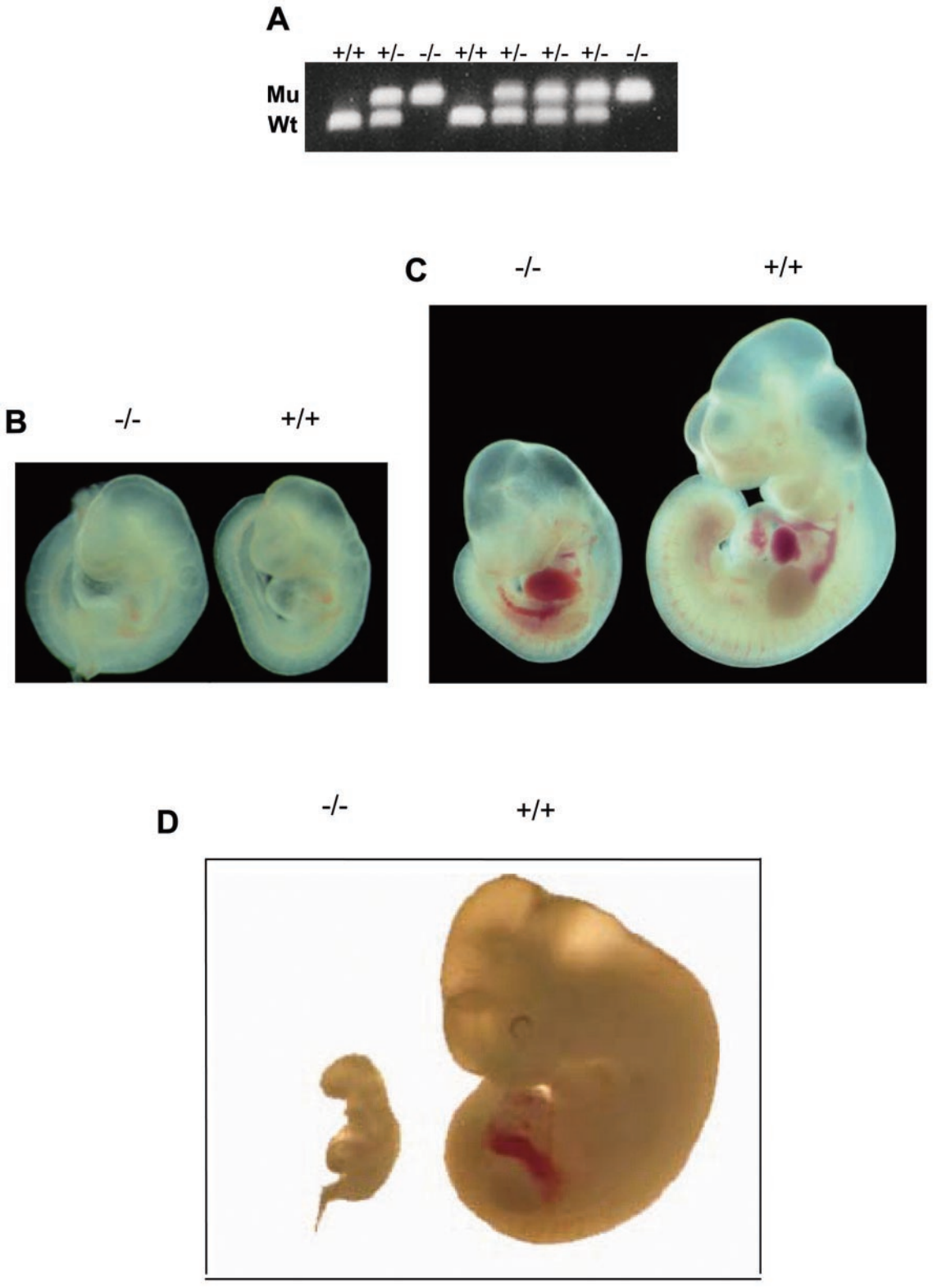

curs, embryos from timed mating between heterozygotes were analyzed at different stages of gestation. The genotype of the embryos was determined by PCR (Fig. 2A). Viable LBP-1a homozygous embryos were obtained with the expected Mendelian frequency at E9.5 and E10.5 (Fig. 1C). Wild-type and LBP-1a-null embryos showed identical development at E9.5 (Fig. 2B). In contrast, LBP-1a$^{-/-}$ embryos at E10.5 were significantly smaller in size in comparison to their wild-type

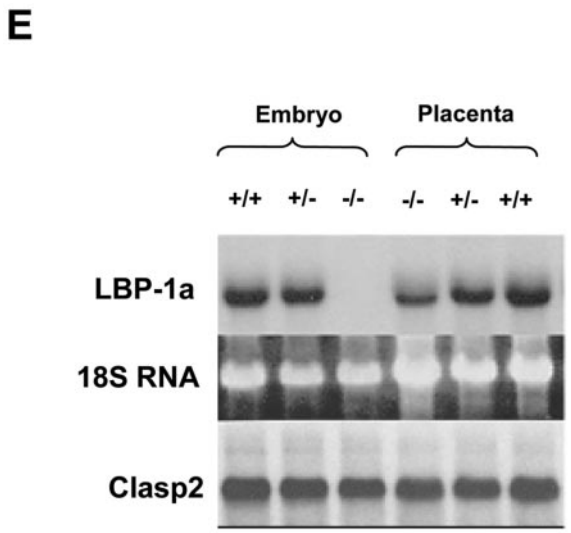

FIG. 2. Embryonic lethality occurs immediately after E10.5 (A) Genomic PCR analysis of littermates derived from a heterozygous intercross harvested at E10.5. The primers utilized and conditions of PCR are provided in Materials and Methods. (B) Macroscopic analysis of LBP-1a-null (−/−) and wild-type (+/+) animals at E9.5 gestation. (C) Macroscopic analysis of LBP-1a-null (−/−) and wild-type (+/+) animals at E10.5 gestation. Note that fetal heartbeats were observed in all mutant and wild-type animals examined. (D) Macroscopic analysis of LBP-1a-null (−/−) and wild-type (+/+) embryos at E11.5 gestation. Note that fetal heartbeats were not observed in the mutant embryos. (E) Expression analysis of the mutated LBP-1a allele. Northern analysis of total RNA isolated from wild-type (+/+), heterozygous (+/−) and homozygous (−/−) animals by using cDNA probes for LBP-1a and CLASP2 genes. Note the uniform transcript level of the CLASP2 gene with all genotypes. Ethidium bromide-stained 18S rRNA was utilized as the loading control. The signal for LBP-1a in the placental samples is indicative of contamination with maternal tissue.

(+/+) littermates (Fig. 2C). Careful morphological examination revealed no structural abnormality, but development was retarded by at least 0.5 days in all instances. At E11.5, the Mendelian frequency of LBP-1a$^{-/-}$ embryos was not reduced significantly, but all mutant embryos were dead, as judged by their necrotic appearance, evidence of resorption, and absence of a fetal heartbeat (Fig. 2D). No LBP-1a homozygous embryos were recovered beyond E11.5.

To confirm that generation of homozygous LBP-1a mutant alleles resulted in a complete loss of expression of an LBP-1a-specific transcript, RNA was harvested from littermates at the E9.5 time point. Northern analysis confirmed that LBP-1a was expressed in wild-type (+/+) and heterozygous (+/−) animals (Fig. 2E). In contrast, embryos that were homozygous for the LBP-1a mutant allele had no evidence of LBP-1a expression utilizing probes specific for the 5′ and 3′ portions of the transcript (Fig. 2E and data not shown). Similar studies of gene expression utilizing reverse transcription-PCR (RT-PCR) analysis with LBP-1a-specific primers confirmed the lack of expression in homozygous LBP-1a-null embryos (data not shown). To exclude a potentially repressive effect of the neomycin phosphotransferase-expressing cassette on adjacent genes, the expression of CLASP2, a ubiquitously expressed factor whose genomic locus is 5′ to the LBP-1a gene, was determined in LBP-1a$^{+/+}$ and LBP-1a$^{-/-}$ animals. CLASP2 expression was unchanged, confirming the specificity of the effects of LBP-1a gene disruption (Fig. 2E, lower panel). In addition, CP2 expression was comparable in wild-type and LBP-1a$^{-/-}$ mice (data not shown), excluding the possibility that the LBP-1a$^{-/-}$ phenotype was the result, at least in part, of coincident dysregulation of CP2 expression. We also considered the possibility that the discrepancy between the CP2 and LBP-1a-null phenotypes reflects differences in unlinked genetic modifiers in the two strains. Several knockout phenotypes, including those with extraembryonic defects, have significant variability in penetrance on different murine backgrounds (37). However, the CP2$^{+/-}$ and LBP-1a$^{+/-}$ strains have been backcrossed onto the C57/B6 strain for multiple generations with no evidence of phenotypic alteration in homozygous offspring.

LBP-1a-null embryos have no focal histological defect. To determine whether an intrinsic embryonic defect might explain the growth retardation and lethal phenotype, macroscopic, histological, and immunohistochemical analysis was performed. At E9.5, LBP-1a-null embryos revealed no abnormality of major organ systems, the body axis or the numbers of somites present (data not shown). Furthermore, the process of embryo turning, a key developmental milestone, was completed in mutant embryos. In contrast, at E10.5, generalized growth retardation was evident in all LBP-1a-null embryos (Fig. 2C and 3A). Despite extensive analysis of many LBP-1a$^{-/-}$ embryos, the only focal gross abnormality observed frequently was a dilated pericardial sac consistent with hemodynamic insufficiency.

Given a potential primary role of a defect in the intraembryonic vasculature in the etiology of intrauterine growth retardation, a closer examination of the developing cardiovascular system was performed. Heart development in LBP-1a-null embryos at E10.5 was comparable to the heart of wild-type E10 embryos. This finding was consistent with that observed in other tissues and reflects a generalized retardation in development after E9.5 in LBP-1a-null embryos. This conclusion was confirmed by the normal architecture of the cardiac atria and ventricles in a majority of the LBP-1a$^{-/-}$ embryos, the myocardial and endocardial layers showing normal trabeculation and endothelial lining (Fig. 3B). Fetal heartbeats were observed up to E10.5 in all embryos examined. However, occasional homozygous embryos were also observed (<10%) with dilated cardiac chambers, a thinned myocardial layer, and reduced trabeculations (data not shown).

The dorsal aortae, major arterial vessels at this stage of gestation were of similar caliber and structure in wild-type and mutant embryos as examined by microscopy and staining with vascular anti-smooth muscle actin antisera (α-SMA) (Fig. 3C). To examine the overall structure of the intraembryonic vasculature, we utilized whole-mount immunohistochemistry with PECAM (Fig. 3D). Similar to immunohistologic analysis with another endothelial specific marker VEGF-R2 (Fig. 3E), we observed no defect in the structure or endothelial lining of embryonic vessels in LBP-1a$^{-/-}$ animals.

An alternate hypothesis to explain the growth retardation is that LBP-1a-null embryos have a defect in primitive erythropoiesis, given that effective distribution of oxygen is critical after E9.5 in the developing fetus. To exclude such a deficiency, we examined hematopoiesis in LBP-1a-null embryos.

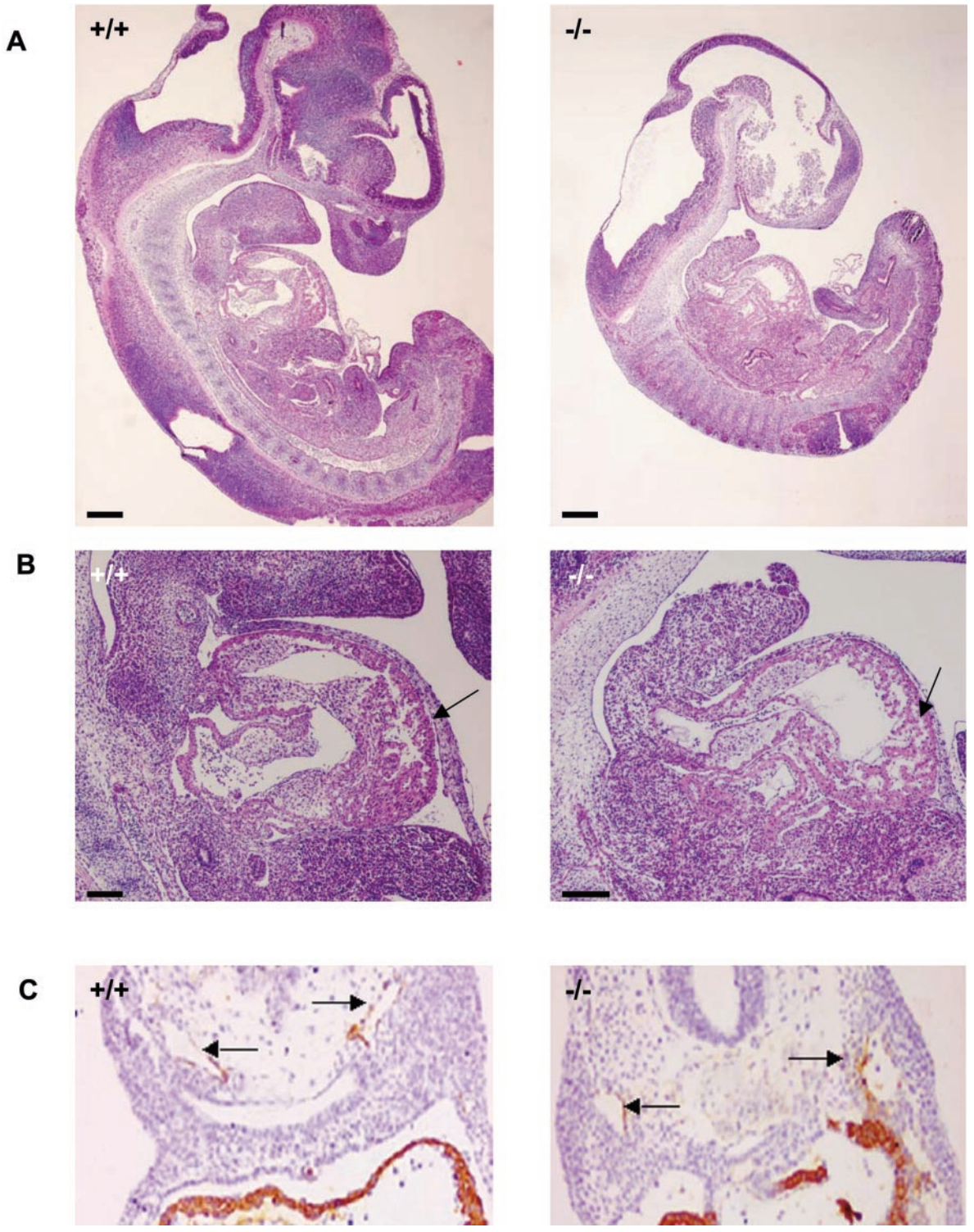

FIG. 3. Normal development but growth retardation in E10.5 LBP-1a$^{-/-}$ embryos. (A) Representative sagittal sections of wild-type (+/+) and LBP-1a-null (−/−) embryos stained with H&E, showing no abnormality in the neural or cardiovascular system. (B) Histological sections of the heart of E10.5 wild-type (+/+) and mutant (−/−) embryos demonstrating the presence of myocardial and endocardial layers and endothelial lining. The myocardial thickness in E10.5 mutant embryos is comparable to that of E10 wild-type embryos, a manifestation of growth retardation after E9.5. An arrow indicates the ventricular myocardial wall. Note the presence of primitive erythroblasts in the heart and adjacent blood vessels of the mutant embryo, a finding consistent with normal primitive hematopoietic differentiation. (C) α-SMA-stained histological sections of the dorsal aortae of E10.5 wild-type (+/+) and mutant (−/−) embryos demonstrating the presence of normal intraembryonic angiogenesis. (D) Whole-mount immunostaining of wild-type (+/+) and mutant (−/−) embryos with the endothelial specific marker PECAM-1 at E10.5 revealing a normal vascular network, regardless of the genotype. (E) VEGF-R2 immunostaining of wild-type (+/+) and mutant (−/−) embryo sections at E10.5 revealing a normal structure and endothelial lining of the major vessels.

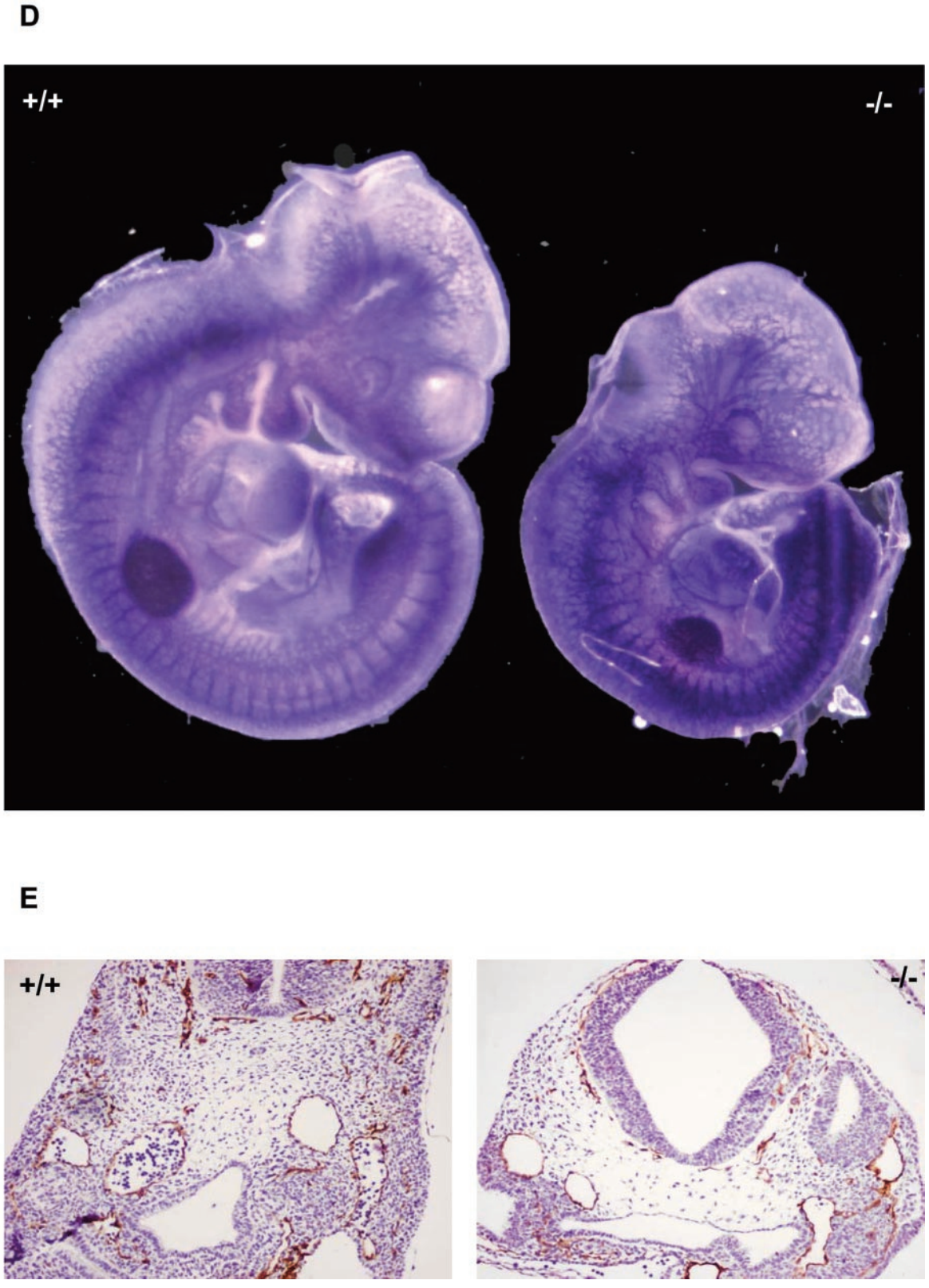

FIG. 3—*Continued*.

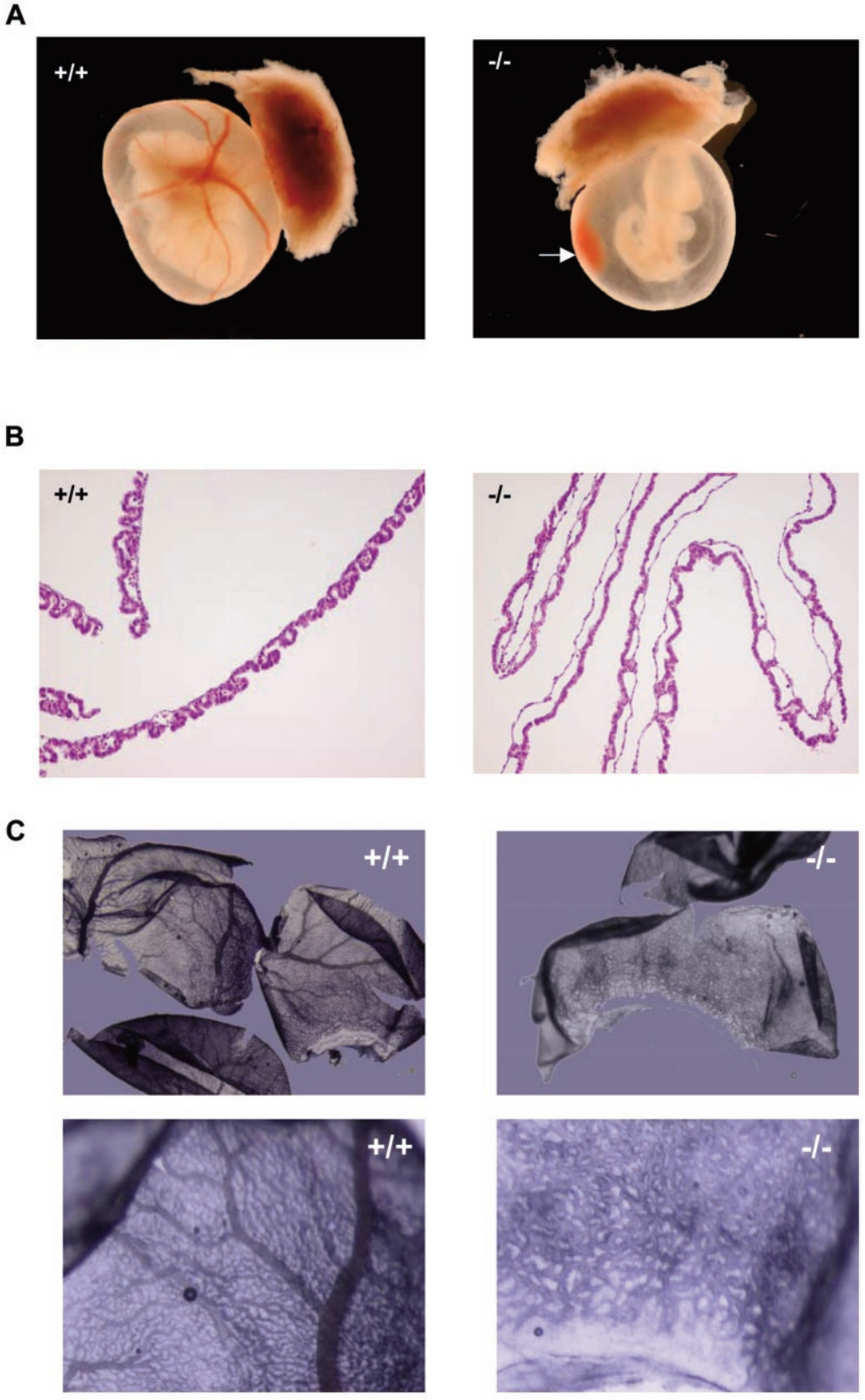
A
+/+
-/-
B
+/+
-/-
C
+/+
-/-
+/+
-/-

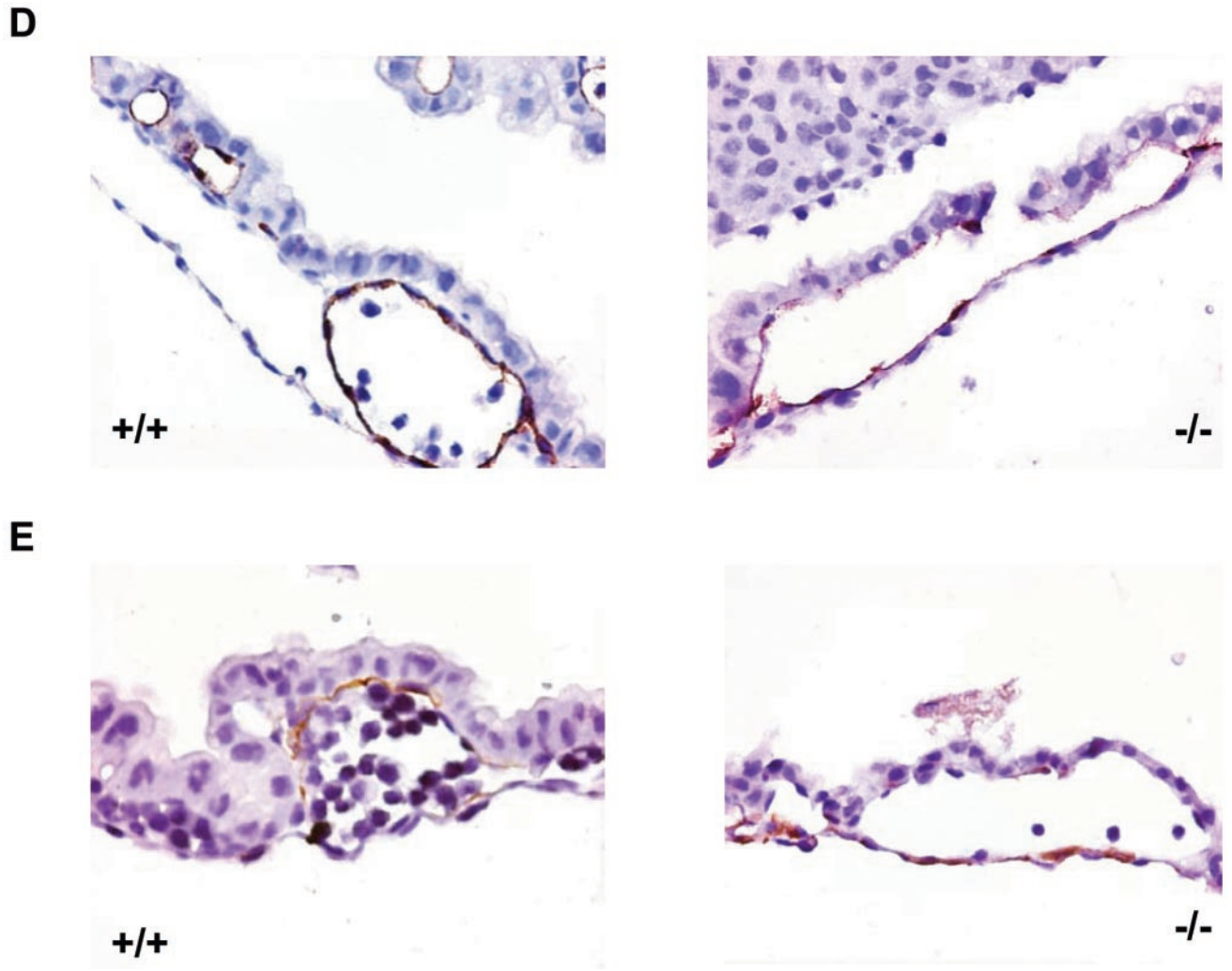

FIG. 4. Yolk sac vascular defect in LBP-1a$^{-/-}$ concepti. (A) Yolk sac of E10.5 wild-type (+/+) and mutant (−/−) embryos with attached placenta. Yolk sacs of mutant embryos were significantly smaller, paler, and lacked large branching vitelline vessels. Note blood collection in yolk sac (arrow). (B) Histological analysis of visceral yolk sac vasculature from E10.5 wild-type (+/+) and mutant (−/−) embryos. Note abnormally dilated capillaries in the mutant yolk sac. (C) Whole-mount immunostaining of E10.5 wild-type (+/+) and mutant (−/−) yolk sacs with the endothelial specific marker VEGF-R2 to demonstrate the absence of large vitelline vessels but a normal capillary network. (D) VEGF-R2 immunostaining of wild-type (+/+) and mutant (−/−) yolk sac sections demonstrating the presence of endothelial cells. Note the sparser and thinned- out endothelial cells in the mutant yolk sac. (E) α-SMA immunostaining of wild-type (+/+) and mutant (−/−) yolk sac sections demonstrating the normal presence of vascular smooth muscle cells in the vessel walls.

Intraluminal fetal erythrocytes of normal morphology were present in the heart and embryonic blood vessels of LBP-1a$^{-/-}$ embryos, albeit in modestly decreased numbers compared to wild-type littermates. In addition, there was no significant difference in the numbers of primitive erythroid progenitors, as measured by CFU-C assays between littermates (data not shown). Taken together, our results suggest that no convincing primary intraembryonic pathology can explain the intrauterine growth retardation and premature lethality in LBP-1a$^{-/-}$ embryos.

LBP-1a deletion results in defective yolk sac vascularization. An alternate explanation for the severe growth retardation observed is a defect in yolk sac and/or placental function. Characterized by the death of embryos at midgestation, defects in these tissues reflect an absolute requirement for a mature placenta, its connecting allantoic or umbilical vessels, and a complex yolk sac vasculature to supply maternally derived nutrients and O_2 to the rapidly developing fetus after E9 (35). To explore this possibility, we examined placental and yolk sac morphology at E8.5, E9.5, and E10.5 of gestation. At the earlier time points, no abnormalities were observed. Specifically, blood islands were formed in the visceral yolk sac, a finding consistent with an intact mechanism of extraembryonic vasculogenesis, and trophoblast giant cell differentiation and ectoplacental cone formation were preserved (data not shown). In contrast to these earlier time points, two striking abnormalities were observed on visual inspection of LBP-1a$^{-/-}$ concepti at E10.5: (i) the complete absence or severe reduction of the extensive vascular network and large vitelline vessels characteristic of the mature visceral yolk sac (Fig. 4A) and (ii) pools

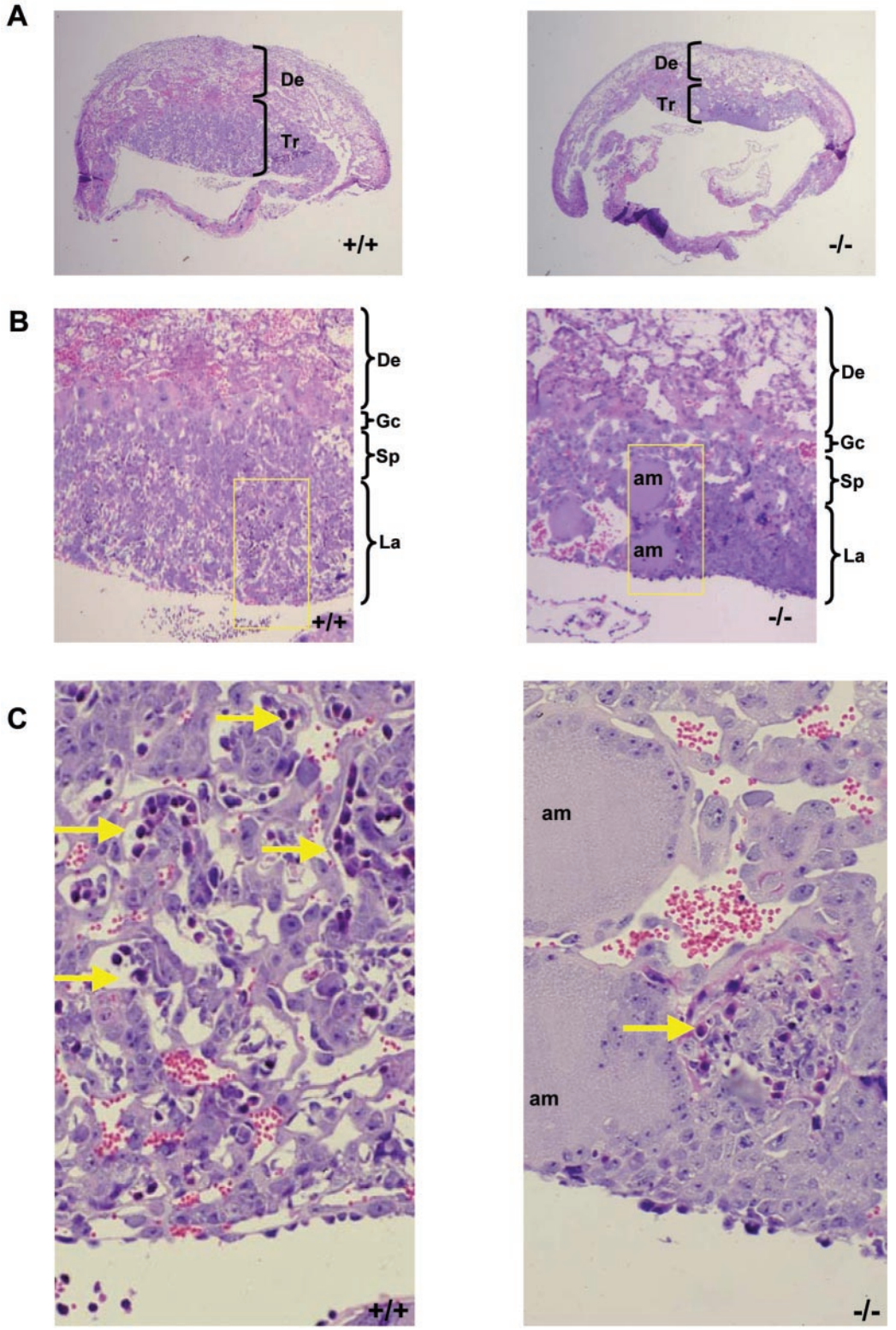

FIG. 5. Defective labyrinthine layer architecture of LBP-1a$^{-/-}$ placenta. (A) H&E-stained sections of E10.5 wild-type (+/+) and mutant (−/−) placenta. De, maternal decidua; Tr, trophoblastic layer. (B) H&E-stained sections of wild-type (+/+) and mutant (−/−) placenta at E10.5 at higher magnification. Note the significant reduction in the labyrinthine layer of the mutant placenta compared to its wild-type littermate. Note the presence of amorphous material. Gc, giant cell layer; Sp, spongiotrophoblast layer; La, labyrinthine trophoblast layer; am, amorphous material. (C) Higher-power magnification of the marked areas in panel B. Arrows denote the embryonic vessels with embryonic erythrocytes. Note the intricate labyrinthine vascular network in the wild-type placenta showing juxtaposition of maternal sinuses with embryonic vessels. Such a pattern is absent altogether in the mutant placenta with allantoic vessels arrested in the lower part of labyrinth. (D) VEGF-R2 immunostaining of E10.5 wild-type (+/+) placenta confirm extensive branching of the allantoic vessels in the labyrinthine layer. (E) VEGF-R2 immunostaining of E10.5 mutant (−/−) placenta show presence of initial penetration of the allantoic vessels but arrest of further branching.

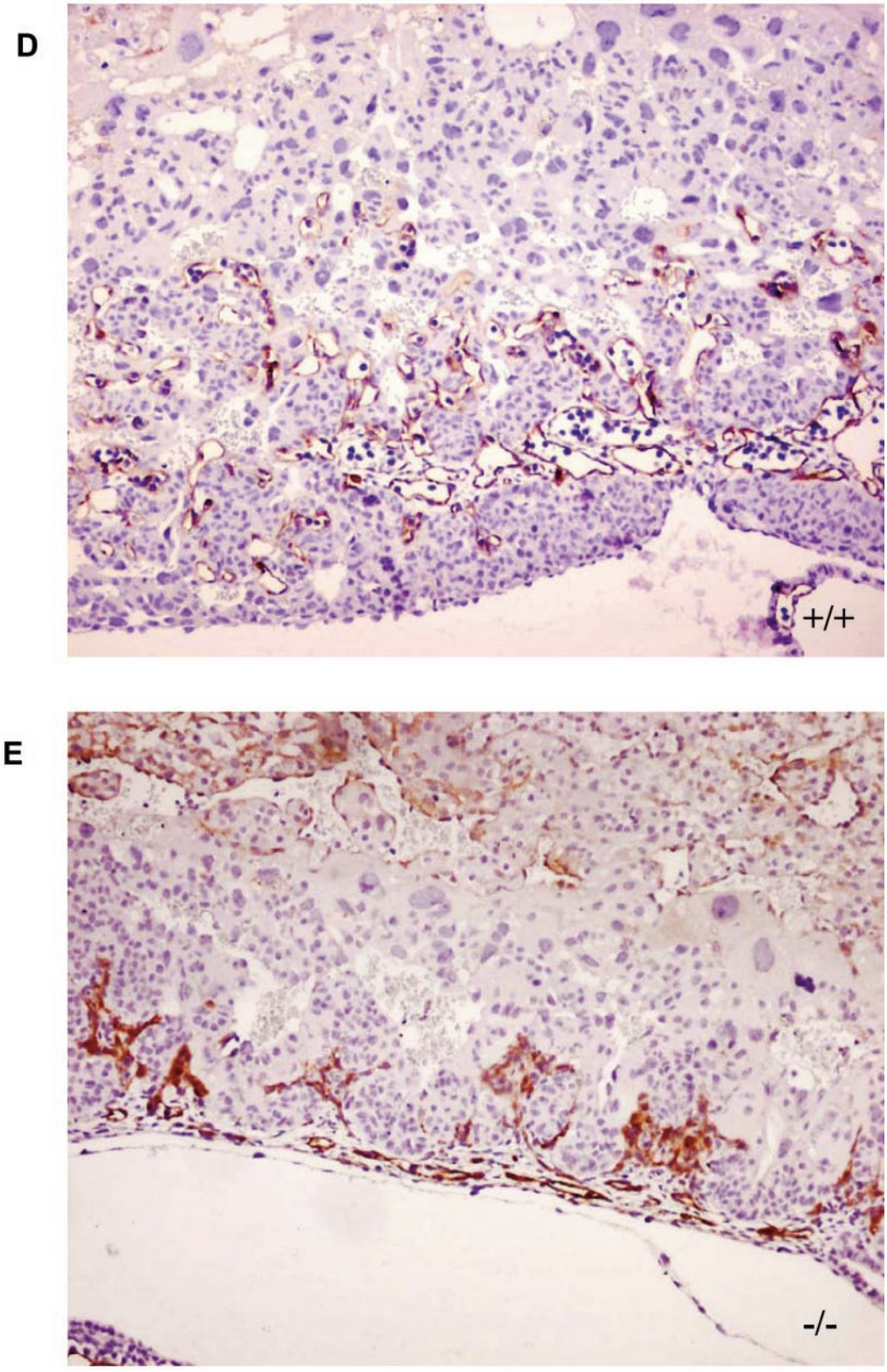

FIG. 5—*Continued*.

of free fetal blood in the amniotic cavity (Fig. 4A, arrow) with no evidence of intraembryonic hemorrhage. This latter observation is seen frequently with defective angiogenesis and has been related to a defect in the structural integrity of the vessel wall (10, 23).

Histologic analysis of the yolk sacs derived from LBP-1a$^{-/-}$ embryos at E10.5 revealed a disorganized vascular pattern. The normally small well-circumscribed vessels with tight endothelial cell lining is characteristic of a wild-type visceral yolk sac being replaced with large vessels with thinner walls and a sparse endothelial cell lining in the LBP-1a mutants (Fig. 4B). Interestingly, the mesodermal layer showed breaks at several points that were consistent with the presence of fetal blood in the amniotic cavity. These findings are characteristic of appropriate initiation of vasculogenesis but failure of angiogenesis. Support for this conclusion was provided by whole-mount immunostaining of yolk sac vasculature with the endothelial marker, VEGF-R2, which showed the presence of endothelial-cell-lined capillary tubes in mutant yolk sacs but little evidence of the intricate network of branching large vitelline and small vessels characteristic of wild-type yolk sacs (Fig. 4C). To confirm this observation, we stained the yolk sac sections with endothelial (VEGF-R2) and vascular smooth muscle (α-SMA) cell-specific antisera (Fig. 4D and E). Mutant and wild-type yolk sacs showed the presence of endothelial and vascular smooth muscle cells but a disorganized vascular architecture in mutant yolk sacs, confirming the presence of an angiogenic, rather than a vasculogenic, defect.

LBP-1a deletion results in defective placental vascularization. Defective yolk sac vascular development has been associated with concomitant defects in the placental vasculature. To determine whether similar abnormalities occur in LBP-1a-null placentas, we examined wild-type, heterozygous, and homozygous placentas from E7.5 through E11.5. Normal placentation was observed in wild-type and heterozygous concepti at all stages of development (data not shown). Similarly, no significant abnormality in LBP-1a$^{-/-}$ placentas was observed at E7.5 to E9.5, the chorionic plate having collapsed onto the underlying ectoplacental cone with chorioallantoic fusion and initiation of vascular penetration (data not shown). In contrast, at E10.5 the LBP-1a$^{-/-}$ placentas showed a significant decrease in the thickness of the labyrinthine layer, with normal giant cell and spongiotrophoblast layers (Fig. 5A and B). Closer examination revealed that the labyrinthine layer of LBP-1a$^{-/-}$ placentas consisted of labyrinthine trophoblasts alone in all instances but lacked the intricate network of branching embryonic vessels characteristic of wild-type placentas (Fig. 5C). Importantly, unlike the wild-type context, fetal blood vessels were not observed in close apposition to maternal blood sinuses in any mutant placenta examined (Fig. 5C, arrows). In addition, large deposits of amorphous material were observed. Interestingly, a previous study on disruption of transcription factor GCMa (3) in mice has also reported presence of amorphous material in largely avascular labyrinth. It was suggested that these collections represent fibrinoid deposits derived from extravasation of blood from a defective vascular bed.

To evaluate the structure of the embryonic vasculature in the placenta more closely, we examined the expression of the endothelial-cell-specific VEGF-R2 antigen. At E10.5, the extensive interdigitating network of VEGF-R2 staining endothelial cells observed within the labyrinthine layer of the wild-type placenta was absent in mutant placentas (compare Fig. 5D and E), thus confirming our histological observations. These results, coupled with the similar disorganized pattern of VEGF-R2 and α-SMA expression in the yolk sac vasculature (Fig. 4), and the normal intraembryonic vasculature (Fig. 3) are consistent with the conclusion that loss of LBP-1a expression results in an extraembryonic angiogenic defect.

Loss of LBP-1a expression does not result in a primary trophoblast defect. Our results provide evidence that loss of LBP-1a expression results in vascular abnormalities of the labyrinthine layer and the yolk sac. However, labyrinthine development is dependent on complex functional interactions between the trophoblast and vascular components. To rule out an unrelated abnormality of trophoblast differentiation as an explanation for the LBP-1a-null placental phenotype, we determined the pattern of expression of key molecular markers by using in situ hybridization riboprobes specific for the three trophoblast cell layers. As shown in Fig. 6A and B, PLF and MPL-1, markers for giant cell trophoblast layer, show similar patterns of expression in normal and mutant placentas at E10.5. A similar result was observed when the expression pattern of the marker 4311 was compared, confirming the integrity of the spongiotrophoblast layer (Fig. 6C). In contrast, HSP-84, a labyrinthine trophoblast specific marker, although expressed, displayed an enhanced intensity compared to the wild-type placenta (Fig. 6D). A result of the compact nature of the mutant placenta, this result suggests that this trophoblast subtype differentiates normally in LBP-1a-null animals. Confirmation of this conclusion was provided by additional in situ hybridization, semiquantitative RT-PCR, and microarray analysis, which confirmed that there was no significant difference in the expression of regulatory factors, such as Esx1 (3, 25, 28) and Dlx3 and Gcm1a (data not shown), previously implicated in labyrinthine trophoblast differentiation.

Functional insights into the etiology of a placental defect are provided frequently by tetraploid complementation assays. In this experiment, wild-type tetraploid embryos are aggregated with the LBP-1a embryos derived from the heterozygous intercrosses to generate chimeric blastocysts. When these blastocysts are transferred to the uteri of pseudopregnant females and allowed to further develop, wild-type tetraploid cells contribute efficiently to the extraembryonic tissues, including the labyrinthine trophoblasts and the visceral endoderm component of the visceral yolk sac. In contrast, they do not contribute to the embryo proper, the extraembryonic mesoderm component of the visceral yolk sac, or the allantoic mesodermal components, including the mesenchyme and the allantoic blood vessels. Thus, if a primary defect resides in the extraembryonic trophoblast-derived component, a normal placental structure should be observed at E10.5 of gestation, and potentially the mutant phenotype should be rescued. After this procedure, 20 pups were delivered by cesarean section at E20.5. These pups had a wild-type or heterozygous genotype only. In contrast, in parallel studies, tetraploid chimeras rescued embryos homozygous for the SOCS3 (45) gene deletion, this gene being associated with a trophoblast-specific defect (data not shown). These results are consistent with either an allantoic mesodermal defect or a secondary developmental block in the

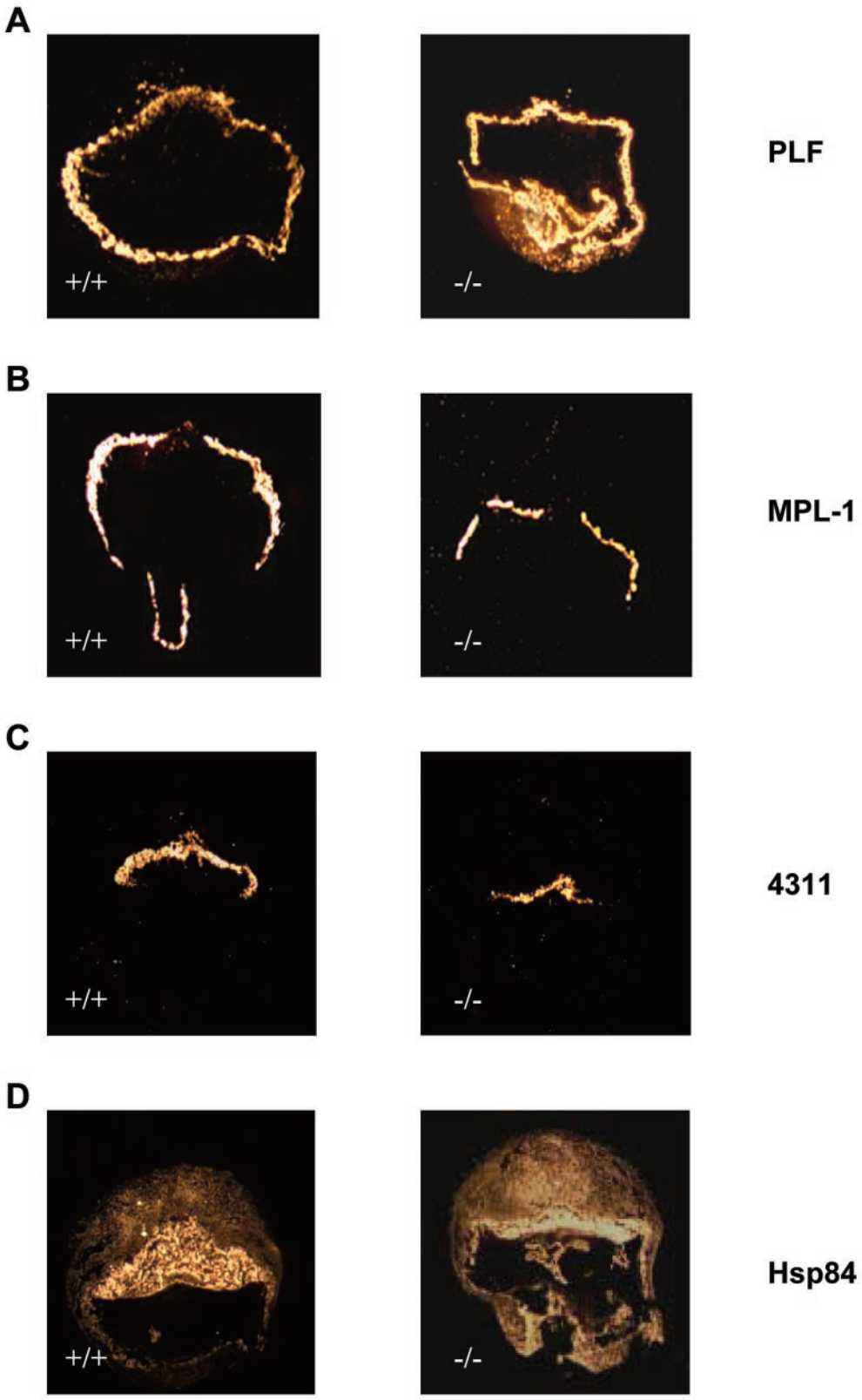

FIG. 6. Normal expression of trophoblast differentiation specific markers in the mutant placenta. (A) The giant cell trophoblast markers PLF is expressed in wild-type (+/+) and mutant (−/−) placentas at E10.5, as assessed by in situ hybridization. (B) The giant cell trophoblast marker MPL-1 is expressed in wild-type (+/+) and mutant (−/−) placentas at E10.5, as assessed by in situ hybridization. (C) Expression of the spongiotrophoblast marker 4311 is present in both strains, suggesting normal differentiation of spongiotrophoblasts. (D) Expression of the labyrinthine trophoblast specific marker HSP-84 is also present in both strains, suggesting normal differentiation of labyrinthine trophoblasts. The apparent enhanced intensity in mutant (−/−) compared to wild-type (+/+) placenta at E10.5 is the result of the compact nature of the labyrinth in the mutant placenta.

A.

Stage	+/+	+/-	-/-	Total
E 10.5	3	3	2	8
E11.5	6	9	2*	17
E12.5	12	21	4*	37
E13.5	2	3	0	5
E14.5	4	7	0	11
E16.5	2	3	0	5
E 18.5#	8	12	0	20

B.

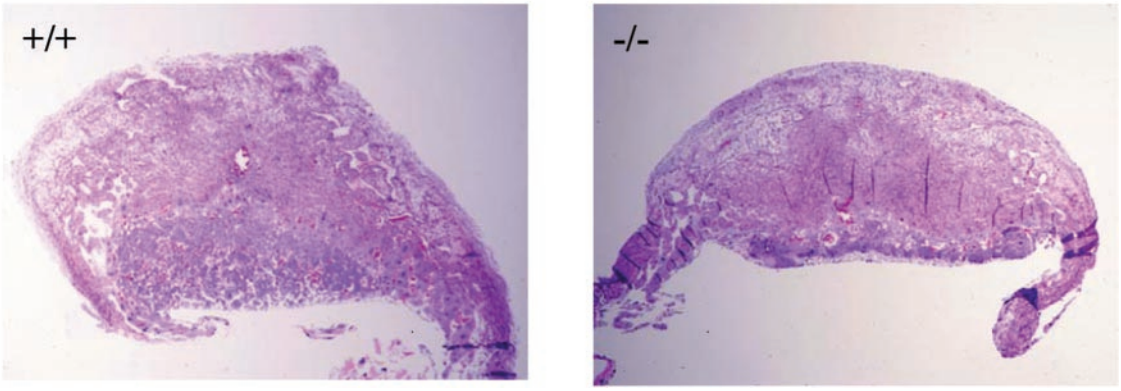

FIG. 7. Tetraploid complementation of the placental trophoblastic component fails to ameliorate the LBP-1a$^{-/-}$ phenotype. (A) Genotyping statistics after tetraploid rescue experiments indicate persistent embryonic lethality after E 10.5 in homozygous mutants. An asterisk indicates dead and necrotic embryos. The number symbol indicates cesarean section. (B) Underdeveloped labyrinthine layer persists in the placenta of mutant (−/−) embryos compared to the placenta of a heterozygous (+/−) embryo after tetraploid assay, suggesting a nontrophoblastic origin of the placental defect.

tetraploid rescued LBP-1a embryos resulting in a late embryonic lethality.

To discriminate between these possibilities, we isolated embryos and placentas at different gestational time points in several tetraploid complementation experiments (Fig. 7A). LBP-1a homozygous embryos derived from these experiments died at a similar time to those generated in heterozygous intercrosses (compare Fig. 1C and 7A). Given that generation of tetraploid chimeras requires a 2-day-old embryo culture period with a resultant delay in development, we observed dead embryos at up to E12.5. Histological examination of the placentas of LBP-1a$^{-/-}$ embryos at E10.5 and E11.5 showed that the tetraploid complementation does not correct the labyrinthine defect (Fig. 7B). The labyrinth in these placentas showed a similar absence of a branching vascular network. Consistent with this result, the yolk sacs derived from homozygous mutant embryos showed a vasculopathy similar to that observed after heterozygous matings (data not shown). Taken together, our findings indicate that normal chorioallantoic placental formation cannot proceed in LBP-1a$^{-/-}$ embryos due to a defect in an allantoic mesodermal component required for extraembryonic angiogenesis.

DISCUSSION

This study provides the first genetic evidence that a member of the mammalian grainyhead transcription factor family is essential for normal extraembryonic vascular development. LBP-1a deficiency results in lethality at midgestation. This result was somewhat surprising, given previous observations of a lack of an abnormal phenotype in animals in which CP2, the highly related orthologue of LBP-1a, was disrupted by homologous recombination. We hypothesized that the outcome in CP2-null animals was a result of functional redundancy, with

LBP-1a substituting for CP2. A similar lack of an abnormal phenotype in LBP-1a-deficient animals might be expected, given the almost identical pattern of gene expression during development, and the similar affinities of the two factors for their cognate DNA regulatory motif. However, the results presented here are consistent with a critical, nonredundant role for LBP-1a during murine development.

A striking abnormality in LBP-1a-null embryogenesis is the lack of appropriate development of the yolk sac and placental vasculature. Our results suggest that this defect results from a perturbation of angiogenesis rather than a vasculogenic defect. Yolk sac vasculogenesis normally precedes placental labyrinth formation. Unlike the LBP-1a phenotype, primary defects in yolk sac vasculogenesis often result in embryonic lethality by E9.5. Moreover, defects in vasculogenesis may affect the intra- and extraembryonic vasculature and primitive hematopoiesis, given the common hemangioblast origin of the endothelium and the blood (8). In the context of LBP-1a deficiency, appropriate development of the cardiovascular system, the formation of blood islands in the visceral yolk sac, and the presence of appropriately differentiated endothelial cells in the primary capillary network suggest no significant defect in intraembryonic hemangioblast differentiation. However, we observed a lack of homogeneity in the diameter of the primary capillary network and a sparse distribution of endothelial cells, findings potentially consistent with a subtle vasculogenic defect. Interestingly, the numbers of erythroid progenitors was normal in LBP-1a embryos, a finding consistent with appropriate differentiation of the LBP-1a-null hemangioblast. These latter observations, coupled with a lack of effect of loss of LBP-1a on primitive globin chain expression (data not shown), confirm that LBP-1a deficiency alone has no effect on erythropoiesis. Given the studies of ourselves and others demonstrating a key role for CP2 and/or LBP-1a in the regulation of the murine and human α- and β-globin gene clusters (26, 55; X. Wang, S. M. Jane, and J. M. Cunningham, unpublished data), it will be instructive to assess the effects of compound homozygosity on developmental erythropoiesis.

In contrast to these findings, there is a marked defect in extraembryonic angiogenesis in LBP-1a-null animals with histological and immunohistochemical evidence of absence of yolk sac vitelline vessels, absence of a mature vascular network, and defective branching morphogenesis of the endothelial cell tubes in LBP-1a deficient placentas. At this time, we cannot discern whether the endothelial cell or the perivascular mesenchyme is the primary cell type affected by loss of LBP-1a expression. The target gene(s) of LBP-1a action remains unclear, given that initial microarray surveys of the expression of key modulators of extraembryonic angiogenesis comparing wild-type and mutant yolk sac tissues demonstrated no significant differences in growth factor or growth factor receptor expression (data not shown). These observations suggest that LBP-1a may be a downstream effector of one or more growth factor pathways. An alternative conclusion is that we may have failed to identify the appropriate factors for study, given the complex array of effectors required for normal angiogenesis (38). Thus, examination of the phenotypes of other gene-targeted murine strains may provide some clues. Attractive candidates include the TGF-β/BMP superfamily, given the known role of *Drosophila grh* in modulating signaling of TGF-β's *Drosophila* homologue decapentaplegic (18) and the similarity of knockouts of members of the TGF-β pathway and LBP-1a-null mice (7, 10, 23, 31). However, comparative microarray analysis and semiquantitative RT-PCR assays evaluating the expression of several TGF-β/BMP ligands, their receptors, and downstream regulatory targets (7, 10, 54) have not shown any significant differences in expression of these factors between wild-type and LBP-1a$^{-/-}$ embryos or yolk sac tissues (V. Parekh and J. M. Cunningham, unpublished data). Indeed, we have recently observed that other ectoderm-specific *Xenopus* orthologues of *Drosophila grh* may be downstream targets of the TGF-β/BMP signaling cascade, suggesting that LBP-1a may act in a similar manner (J. Tao and J. M. Cunningham, unpublished data). Alternatively, a labyrinthine vascular defect similar to LBP-1a deficiency is also observed with disruption of FGF signaling (17). FGF ligands have also been implicated in the regulation of epithelial branching in the lung, kidney, and trachea (14, 44, 50). Moreover, recent studies suggest that FGF control of branching morphogenesis in *Drosophila* is dependent on intact *grh* function (17). Given the defect in labyrinthine branching morphogenesis observed here, it will be important to determine whether there is a similar linkage in mammals. Together, our observations provide an initial basis to explore the growth factor signaling pathways that may regulate LBP-1a expression or function during murine extraembryonic angiogenesis.

A third key feature of the LBP-1a$^{-/-}$ phenotype is the defect in vascularization of the chorioallantoic labyrinth. Lack of effective placental angiogenesis may result from a primary failure of syncytiotrophoblast differentiation, an allantoic mesenchymal or vascular deficiency or defective cell-cell signaling. Deficiency of ARNT, a member of the basic helix-loop-helix/PAS family of transcription factors, results in a similar failure of allantoic invasion and branching to that observed in the LBP-1a-deficient embryos (22). The yolk sac vasculature is apparently normal in this context, and the defect is rescued by tetraploid complementation, suggesting a primary trophoblast deficiency. Loss of the mesenchymal or endothelial components of the allantois can, similar to LBP-1a deficiency, also cause a secondary loss of labyrinthine architecture, as observed with loss of expression of Hsp84-1 (49) and several vascular growth factors. However, given the ubiquitous nature of LBP-1a expression, it is possible that coincident defects in the chorionic trophoectoderm and allantoic mesoderm are necessary for generation of the mutant phenotype. In an attempt to discriminate between these models, we utilized two complementary approaches: trophoblast differentiation marker expression analysis and tetraploid complementation. The former assay confirmed that all three cell types derived from the trophoblastic stem cell differentiated normally. Tetraploid aggregation studies failed to rescue the chorionic placental defects, supporting the conclusion that an allantoic vasculature defect is the primary cause of the LBP-1a phenotype. These observations add LBP-1a to the list of factors necessary for allantois development. Further studies will be necessary to establish the linkage, if any, between the roles played by these factors and that of LBP-1a in allantoic differentiation.

The rapidity of onset and the severity of the intrauterine growth retardation after E9.5 is a striking feature of LBP-1a-deficient embryos. Histological analysis failed to identify a

consistent intraembryonic focal defect that could account for the lethality. However, we cannot exclude a subtle defect in the embryonic cardiovascular system, given that a small proportion of embryos have thinned ventricular walls. However, it is unclear at this time whether this is a direct effect of LBP-1a deficiency or whether it relates to the growth retardation inherent to the mutant phenotype. A more direct approach to addressing this issue will be provided by an LBP-1a conditional knockout mouse strain that is currently being developed.

Given the ubiquitous nature of LBP-1a expression, the null phenotype might be explained by a role for the gene in cell growth and apoptosis. Thus, loss of LBP-1a could result in a generalized cell-autonomous proliferation defect or an increased apoptosis rate. However, this hypothesis is unlikely to be correct given that, until E9.5, LBP-1a$^{-/-}$ embryos are comparable in growth with heterozygous and wild-type littermates. Indeed, determination of in vivo rates of cellular proliferation and apoptosis after E9.5 would be confounded by the compromise of feto-maternal exchange in the mutant embryos, making the determination of a causal relationship inherently difficult. Independent support for the lack of a significant intraembryonic defect in LBP-1a$^{-/-}$ embryos was provided by the microarray analysis, showing lack of significant differences in the expression of known growth and/or apoptosis modulator genes, including those that are known to be regulated by LBP-1a/CP2. We are currently assessing the significance of the changes in expression of other genes identified in our microarray studies, whose modulation by LBP-1a has not been investigated previously. However, we note that a relative expression of many genes is increased in LBP-1a$^{-/-}$ embryos. Although the significance of these changes is at present unclear, our previous finding that CP2 and LBP-1a interact with a polycomb repressor complex (47) suggests that loss of LBP-1a expression may result in derepression of gene expression in some contexts.

Taken together, our studies support the conclusion that the phenotype observed in LBP-1a-deficient mice is related to a defect in extraembryonic angiogenesis. Significant evidence in humans links intrauterine growth retardation with the labyrinthine and vascular defects observed in preeclampsia and missed abortion (34). It will be important to explore if alteration of human LBP-1a expression contributes to the pathogenesis of these disorders.

ACKNOWLEDGMENTS

We thank members of the Cunningham and Jane laboratories for helpful discussions. We thank the Transgenic Core Unit for ES cell injections, Xiuling Li and Jin He for technical assistance, and Alicia Malone for secretarial support.

This study was supported by the National Institutes of Health, the Assisi Foundation of Memphis, the American Lebanese Syrian Associated Charities, the Australian NHMRC, and the Wellcome Trust.

REFERENCES

1. **Adams, R. H., A. Porras, G. Alonso, M. Jones, K. Vintersten, S. Panelli, A. Valladares, L. Perez, R. Klein, and A. R. Nebreda.** 2000. Essential role of p38α MAP kinase in placental but not embryonic cardiovascular Development. Mol. Cell **6:**109–116.
2. **Akhmanova, A., C. C. Hoogenraad, K. Drabek, T. Stepanova, B. Dortland, T. Verkerk, W. Vermeulen, B. M. Burgering, C. I. De Zeeuw, F. Grosveld, and N. Galjart.** 2001. Clasps are CLIP-115 and -170 associating proteins involved in the regional regulation of microtubule dynamics in motile fibroblasts. Cell **104:**923–935.
3. **Anson-Cartwright, L., K. Dawson, D. Holmyard, S. J. Fisher, R. A. Lazzarini, and J. C. Cross.** 2000. The glial cells missing-1 protein is essential for branching morphogenesis in the chorioallantoic placenta. Nat. Genet. **25:** 311–314.
4. **Bray, S. J., and F. C. Kafatos.** 1991. Developmental function of Elf-1: an essential transcription factor during embryogenesis in *Drosophila*. Genes Dev. **5:**1672–1683.
5. **Byrd, N., S. Becker, P. Maye, R. Narasimhaiah, B. St Jacques, X. Zhang, J. McMahon, A. McMahon, and L. Grabel.** 2002. Hedgehog is required for murine yolk sac angiogenesis. Development **129:**361–372.
6. **Carney, E. W., V. Prideaux, S. J. Lye, and J. Rossant.** 1993. Progressive expression of trophoblast-specific genes during formation of mouse trophoblast giant cells in vitro. Mol. Reprod. Dev. **34:**357–368.
7. **Chang, H., D. Huylebroeck, K. Verschueren, Q. Guo, M. M. Matzuk, and A. Zwijsen.** 1999. Smad5 knockout mice die at mid-gestation due to multiple embryonic and extraembryonic defects. Development **126:**1631–1642.
8. **Choi, K., M. Kennedy, A. Kazarov, J. C. Papadimitriou, and G. Keller.** 1998. A common precursor for hematopoietic and endothelial cells. Development **125:**725–732.
9. **Damert, A., L. Miquerol, M. Gertsenstein, W. Risau, and A. Nagy.** 2002. Insufficient VEGFA activity in yolk sac endoderm compromises hematopoietic and endothelial differentiation. Development **129:**1881–1892.
10. **Dickson, M. C., J. S. Martin, F. M. Cousins, A. B. Kulkarni, S. Karlsson, and R. J. Akhurst.** 1995. Defective hematopoiesis and vasculogenesis in transforming growth factor-beta 1 knockout mice. Development **121:**1845–1854.
11. **Dietrich, S., F. Abou-Rebyeh, H. Brohmann, F. Bladt, E. Sonnenberg-Riethmacher, T. Yamaai, A. Lumsden, B. Brand-Saberi, and C. Birchmeier.** 1999. The role of SF/HGF and c-Met in the development of skeletal muscle. Development **126:**1621–1629.
12. **Fong, G. H., J. Rossant, M. Gertsenstein, and M. L. Breitman.** 1995. Role of the Flt-1 receptor tyrosine kinase in regulating the assembly of vascular endothelium. Nature **376:**66–70.
13. **Giroux, S., M. Tremblay, D. Bernard, J. F. Cardin-Girard, S. Aubry, L. Larouche, S. Rousseau, J. Huot, J. Landry, L. Jeannotte, and J. Charron.** 1999. Embryonic death of Mek1-deficient mice reveals a role for this kinase in angiogenesis in the labyrinthine region of the placenta. Curr. Biol. **9:**369–372.
14. **Grisaru, S., D. Cano-Gauci, J. Tee, J. Filmus, and N. D. Rosenblum.** 2001. Glypican-3 modulates BMP- and FGF-mediated effects during renal branching morphogenesis. Dev. Biol. **231:**31–46.
15. **Guillemot, F., A. Nagy, A. Auerbach, J. Rossant, and A. L. Joyner.** 1994. Essential role of Mash-2 in extraembryonic development. Nature **371:**333–336.
16. **Gurtner, G. C., V. Davis, H. Li, M. J. McCoy, A. Sharpe, and M. I. Cybulsky.** 1995. Targeted disruption of the murine VCAM1 gene: essential role of VCAM-1 in chorioallantoic fusion and placentation. Genes Dev. **9:**1–14.
17. **Hemphala, J., A. Uv, R. Cantera, S. Bray, and C. Samakovlis.** 2003. Grainy head controls apical membrane growth and tube elongation in response to Branchless/FGF signalling. Development **130:**249–258.
18. **Huang, J. D., T. Dubnicoff, G. J. Liaw, Y. Bai, S. A. Valentine, J. M. Shirokawa, J. A. Lengyel, and A. J. Courey.** 1995. Binding sites for transcription factor NTF-1/Elf-1 contribute to the ventral repression of decapentaplegic. Genes Dev. **9:**3177–3189.
19. **Ishikawa, T., Y. Tamai, A. M. Zorn, H. Yoshida, M. F. Seldin, S. Nishikawa, and M. M. Taketo.** 2001. Mouse Wnt receptor gene Fzd5 is essential for yolk sac and placental angiogenesis. Development **128:**25–33.
20. **Itoh, M., Y. Yoshida, K. Nishida, M. Narimatsu, M. Hibi, and T. Hirano.** 2000. Role of Gab1 in heart, placenta, and skin development and growth factor- and cytokine-induced extracellular signal-regulated kinase mitogen-activated protein kinase activation. Mol. Cell. Biol. **20:**3695–3704.
21. **Jane, S. M., A. W. Nienhuis, and J. M. Cunningham.** 1995. Hemoglobin switching in man and chicken is mediated by a heteromeric complex between the ubiquitous transcription factor CP2 and a developmentally specific protein. EMBO J. **14:**97–105.
22. **Kozak, K. R., B. Abbott, and O. Hankinson.** 1997. ARNT-deficient mice and placental differentiation. Dev. Biol. **191:**297–305.
23. **Larsson, J., M. J. Goumans, L. J. Sjostrand, M. A. van Rooijen, D. Ward, P. Leveen, X. Xu, P. ten Dijke, C. L. Mummery, and S. Karlsson.** 2001. Abnormal angiogenesis but intact hematopoietic potential in TGF-beta type I receptor-deficient mice. EMBO J. **20:**1663–1673.
24. **Li, D. Y., L. K. Sorensen, B. S. Brooke, L. D. Urness, E. C. Davis, D. G. Taylor, B. B. Boak, and D. P. Wendel.** 1999. Defective angiogenesis in mice lacking endoglin. Science **284:**1534–1537.
25. **Li, Y., and R. R. Behringer.** 1998. Esx1 is an X-chromosome-imprinted regulator of placental development and fetal growth. Nat. Genet. **20:**309–311.
26. **Lim, L. C., S. L. Swendeman, and M. Sheffery.** 1992. Molecular cloning of the alpha-globin transcription factor CP2. Mol. Cell. Biol. **12:**828–835.
27. **Monkley, S. J., S. J. Delaney, D. J. Pennisi, J. H. Christiansen, and B. J. Wainwright.** 1996. Targeted disruption of the Wnt2 gene results in placentation defects. Development **122:**3343–3353.
28. **Morasso, M. I., A. Grinberg, G. Robinson, T. D. Sargent, and K. A. Mahon.** 1999. Placental failure in mice lacking the homeobox gene Dlx3. Proc. Natl. Acad. Sci. USA **96:**162–167.

29. **Ogura, Y., N. Takakura, H. Yoshida, and S. I. Nishikawa.** 1998. Essential role of platelet-derived growth factor receptor alpha in the development of the intraplacental yolk sac/sinus of Duval in mouse placenta. Biol. Reprod. **58:**65–72.
30. **Ohlsson, R., P. Falck, M. Hellstrom, P. Lindahl, H. Bostrom, G. Franklin, L. Ahrlund-Richter, J. Pollard, P. Soriano, and C. Betsholtz.** 1999. PDGFB regulates the development of the labyrinthine layer of the mouse fetal placenta. Dev. Biol. **212:**124–136.
31. **Oshima, M., H. Oshima, and M. M. Taketo.** 1996. TGF-beta receptor type II deficiency results in defects of yolk sac hematopoiesis and vasculogenesis. Dev. Biol. **179:**297–302.
32. **Parr, B. A., V. A. Cornish, M. I. Cybulsky, and A. P. McMahon.** 2001. Wnt7b regulates placental development in mice. Dev. Biol. **237:**324–332.
33. **Ramamurthy, L., V. Barbour, A. Tuckfield, D. R. Clouston, D. Topham, J. M. Cunningham, and S. M. Jane.** 2001. Targeted disruption of the CP2 gene, a member of the NTF family of transcription factors. J. Biol. Chem. **276:**7836–7842.
34. **Regnault, T. R., H. L. Galan, T. A. Parker, and R. V. Anthony.** 2002. Placental development in normal and compromised pregnancies: a review. Placenta **23**(Suppl. A)**:**S119–S129.
35. **Rossant, J., and J. C. Cross.** 2001. Placental development: lessons from mouse mutants. Nat. Rev. Genet. **2:**538–548.
36. **Sambrook, J., D. W. Russell.** 2000. Molecular cloning: a laboratory manual. Cold Spring Harbor Laboratory Press, Cold Spring Harbor, N.Y.
37. **Sanford, L. P., S. Kallapur, I. Ormsby, and T. Doetschman.** 2001. Influence of genetic background on knockout mouse phenotypes. Methods Mol. Biol. **158:**217–225.
38. **Sato, T. N., and S. Loughna.** 2002. Vasculogenesis and angiogenesis, p. 211–233. *In* J. Rossant (ed.), Mouse development. Academic Press, Inc., New York, N.Y.
39. **Schlaeger, T. M., Y. Qin, Y. Fujiwara, J. Magram, and T. N. Sato.** 1995. Vascular endothelial cell lineage-specific promoter in transgenic mice. Development **121:**1089–1098.
40. **Shalaby, F., J. Rossant, T. P. Yamaguchi, M. Gertsenstein, X. F. Wu, M. L. Breitman, and A. C. Schuh.** 1995. Failure of blood-island formation and vasculogenesis in Flk-1-deficient mice. Nature **376:**62–66.
41. **Shirra, M. K., and U. Hansen.** 1998. LSF and NTF-1 share a conserved DNA recognition motif yet require different oligomerization states to form a stable protein-DNA complex. J. Biol. Chem. **273:**19260–19268.
42. **Solloway, M. J., and E. J. Robertson.** 1999. Early embryonic lethality in Bmp5;Bmp7 double mutant mice suggests functional redundancy within the 60A subgroup. Development **126:**1753–1768.
43. **Sueyoshi, T., R. Kobayashi, K. Nishio, K. Aida, R. Moore, T. Wada, H. Handa, and M. Negishi.** 1995. A nuclear factor (NF2d9) that binds to the male-specific P450 (Cyp 2d-9) gene in mouse liver. Mol. Cell. Biol. **15:**4158–4166.
44. **Sutherland, D., C. Samakovlis, and M. A. Krasnow.** 1996. *branchless* encodes a *Drosophila* FGF homolog that controls tracheal cell migration and the pattern of branching. Cell **87:**1091–1101.
45. **Takahashi, Y., N. Carpino, J. C. Cross, M. Torres, E. Parganas, and J. N. Ihle.** 2003. SOCS3: an essential regulator of LIF receptor signaling in trophoblast giant cell differentiation. EMBO J. **22:**372–384.
46. **Ting, S. B., T. Wilanowski, L. Cerruti, L. L. Zhao, J. M. Cunningham, and S. M. Jane.** 2003. The identification and characterization of human Sister-of-Mammalian Grainyhead (SOM) expands the grainyhead-like family of developmental transcription factors. Biochem. J. **370:**953–962.
47. **Tuckfield, A., D. R. Clouston, T. M. Wilanowski, L. L. Zhao, J. M. Cunningham, and S. M. Jane.** 2002. Binding of the RING polycomb proteins to specific target genes in complex with the grainyhead-like family of developmental transcription factors. Mol. Cell. Biol. **22:**1936–1946.
48. **Volker, J. L., L. E. Rameh, Q. Zhu, J. DeCaprio, and U. Hansen.** 1997. Mitogenic stimulation of resting T cells causes rapid phosphorylation of the transcription factor LSF and increased DNA-binding activity. Genes Dev. **11:**1435–1446.
49. **Voss, A. K., T. Thomas, and P. Gruss.** 2000. Mice lacking HSP90beta fail to develop a placental labyrinth. Development **127:**1–11.
50. **Warburton, D., M. Schwarz, D. Tefft, G. Flores-Delgado, K. D. Anderson, and W. V. Cardoso.** 2000. The molecular basis of lung morphogenesis. Mech. Dev. **92:**55–81.
51. **Wilanowski, T., A. Tuckfield, L. Cerruti, S. O'Connell, R. Saint, V. Parekh, J. Tao, J. M. Cunningham, and S. M. Jane.** 2002. A highly conserved novel family of mammalian developmental transcription factors related to *Drosophila* grainyhead. Mech. Dev. **114:**37–50.
52. **Xu, X., M. Weinstein, C. Li, M. Naski, R. I. Cohen, D. M. Ornitz, P. Leder, and C. Deng.** 1998. Fibroblast growth factor receptor 2 (FGFR2)-mediated reciprocal regulation loop between FGF8 and FGF10 is essential for limb induction. Development **125:**753–765.
53. **Yang, J. T., H. Rayburn, and R. O. Hynes.** 1995. Cell adhesion events mediated by alpha 4 integrins are essential in placental and cardiac development. Development **121:**549–560.
54. **Zhang, H., and A. Bradley.** 1996. Mice deficient for BMP2 are nonviable and have defects in amnion/chorion and cardiac development. Development **122:**2977–2986.
55. **Zhou, W., D. R. Clouston, X. Wang, L. Cerruti, J. M. Cunningham, and S. M. Jane.** 2000. Induction of human fetal globin gene expression by a novel erythroid factor, NF-E4. Mol. Cell. Biol. **20:**7662–7672.